Modeling urbanization patterns and morphological evolution of Sargodha city, Pakistan using remote sensing and GIS

Humayun Ashraf*, Saira Munawar

Department of Geography, University of Gujrat, Pakistan

*Corresponding Author e-mail: humayun.22@uog.edu.pk

Received: 26 August 2026 / Accepted: 16 October 2026

Abstract. Rapid urbanization has significantly transformed land use and land cover (LULC) patterns in developing countries, resulting in increasing environmental challenges. This study examines the Spatio-temporal dynamics of LULC change in Sargodha City, Pakistan, from 1992 to 2024 using remote sensing, machine learning, and geospatial modeling techniques. Landsat imagery from 1992, 2000, 2008, 2016, and 2024 was processed in Google Earth Engine (GEE), and LULC classes were classified into urban land, vegetation, water bodies, and barren land using the Random Forest (RF) algorithm. The overall accuracy ranged from 88.27 percent in 1992 to 95.26 percent in 2024, and the Kappa statistics fell within a range of 0.82 to 0.91. Spectral indices including NDVI, NDBI, and NDWI were used to assess environmental changes associated with urban expansion. The results indicate that urban land increased from 131 km² (8.5%) in 1992 to 220 km² (14.23%) in 2024, while vegetation cover declined from 1356 km² (87.7%) to 1259 km² (81.43%). Future LULC changes were simulated using the CA–Markov model, which predicts urban expansion to 351 km² (22.69%) and a reduction in vegetation cover to 1080 km² (69.85%) by 2040. The findings highlight the rapid pace of urban growth in Sargodha City and emphasize the need for sustainable urban planning and land management strategies to reduce environmental degradation and support balanced urban development.

Keywords: Google Earth Engine (GEE), CA-Markov, Random Forest (RF) algorithm, Land Use/Land Cover (LULC), Spatio-Temporal Analysis.

1.Introduction

Cities across the globe grew by about 1.5% each year from 2000 to 2015; in developing countries, city growth was around 2.6% each year (United Nations, 2019). Urban expansion leads to considerable changes in land use/land cover typologies, resulting in several environmental problems (Aylett et al., 2015). The transformation in urban landscapes comes about as a result of population increase and commercial development. Today, over half of the world's population (Gu et al., 2021) has increased, and it is estimated that by 2050, about 68%

of the world's population will be living in urban areas. Urbanization in the form of sprawl significantly affects landscapes (Nuissl & Siedentop, 2021). Due to the transformation of vegetation (Tichý et al., 2020) into urban land, the effects on agriculture by reducing available land potentially lead to food insecurity (Yar & Huafu, 2019). Build-up areas, although small in size, have negative impacts, especially in less developed countries (Gao et al., 2020). In 1995, the International Human Dimensions Program (IHDP) and the International Geosphere-Biosphere Program (IGBP) acknowledged the significance of learning landscape changes (Cao et al., 2020), forming it as a crucial focus in global change exploration (Winkler et al., 2021; Xiang et al., 2022). In Pakistan, the population growth rate is approximately 3%, and currently, one-third of the nation's population resides in urban areas (A. Aslam, 2024).

Agriculture is a key component of Pakistan's economy and contributes 22.4% of the GDP (Jatoi, 2021). However, Urban expansion effects on agriculture and other landscape features lead to environmental issues (Hussain et al., 2022). Effective urban planning and sustainable land management areas are important (Butt et al., 2015). Between 2001 and 2020, about 1.9% of Pakistan's land degraded due to human activity (Peng et al., 2023). In Sargodha rapid urban growth reduced vegetation from 80% to 71%, while urban areas increased from 5% to 21 % (Sameer et al., 2025). The city experienced a 41.9% increase in population density from 1992 to 2017 (Farooq et al., 2024). However, rapid urbanization affects biodiversity and ecosystems (Hashim et al., 2023). Remote sensing (RS) (Khanal et al., 2020) and GIS enable the collection of multi-spectral and multi-temporal data, which is useful in marking changes in landscapes (Kabisch et al., 2019). As cities spread, greenery and water sources shrink, addressing environmental concerns (Jothimani et al., 2021). Vegetation index and normalized differential index are useful indicators for vegetation and water health (Tassi & Vizzari, 2020), parameters include, the normalized vegetation index (NDVI) (Huang et al., 2021) and normalized differential index (NDBI) Normalized Water Index (NDWI) (Guha et al., 2020; Jaber, 2021). CA Markov (Fu et al., 2022; Zhou et al., 2020) model is used for the prediction of landscape data. This model effectively simulated LULC changes, highlighting significant land cover transitions. These insights support sustainable land management and urban planning for future development (Mansour et al., 2020). land is utilized, the environment invariably suffers the consequences. Better land management strategies to mitigate this issue and keep nature in check are needed (Hailu et al., 2020).

In the Gorgan River Basin, according to (Yaghoobi et al., 2022), deforestation, rangeland degradation, and agricultural activities have been observed between 1990 and 2020. The report (Naikoo et al., 2020)analyzes and forecasts through models of LULC. While emphasizing the hybrid models' potential for urban development and ecological land planning. According to a research paper, Delhi NCR has experienced significant shifts in LULC patterns, including a 326% increase in construction at the loss of green and agricultural land (Verma et al., 2020). Moving populations are transforming the way we use and cover land, and investigating and devising strategies to reduce these effects. It's particularly critical for cities that are under a bigger threat (Chen et al., 2020).

This study concluded that changes in Melbourne LULC between 2001 and 2018 increased in the midday time of 5.1°C, the classification of LULC, with NDBI (Jamei et al., 2022). A study concludes that Google Earth Engine (GEE) is an effective tool for analyzing urbanization in Mawlamyine City using NDVI, NDWI, and NDBI in Landsat data (Khine et al., 2018). A study of the rapid expansion of cities in the district of Lahore (1992) resulted in a 30.4% increase in regional growth and a 196.5% increase in vegetation, and a 30.4% increase (Farhan et al., 2024). Another study takes a journey through time to explore how land use and cover have changed in Meherpur, Bangladesh, and what the future may hold (Hossain & Rahman, 2024). The focus is on the Ajay River watershed, examining both past trends and possible future developments. To assist in better planning, it employs RF classification and CA-Markov modeling (Roy et al., 2024). The research looks at shifts in land use and cover, addresses the issue of urban sprawl, and predicts future scenarios using satellite images along with CA-Markov modeling. (Manna et al., 2024). This research gave us estimates of soil erosion and sediment yield while considering expected changes in LULC. These findings will help promote better land management practices and support agricultural planning efforts (Sampath & Radhakrishnan, 2024). A paper investigates historical and projected LULC alterations in Kano Metropolis through the application of Geographic Information Systems (GIS) alongside a Cellular Automata-Markov (CA-Markov) model (Koko et al., 2022).

This study has put particular emphasis on the changes in vegetation cover in Sargodha City owing to its ecological importance and its vulnerability to rapid urbanization. In this way, the study tries to determine the extent of vegetation loss and its spatial pattern in association with urbanization through the use of NDVI and LULC analysis. In this way, the methodology

adopted here has made it possible to understand the link between urbanization and the changes in vegetation cover. These studies analyze the urban sprawl for the Sargodha City by using Landsat imagery available from 1987 to 2017 and found an urban area increased by 244.4 percent along with the rise in land surface temperatures (Ashraf et al., 2023). The findings substantiate the policymakers in terms of sustainable planning of cities for better living conditions, as such research studies track urban sprawl in Sargodha City (1987-2017) using remote sensing and statistical analysis to show conversion of land uses (Ashraf et al., 2022).The capabilities of Google Earth Engine (Zhao et al., 2021) allow for the development of land use/land cover data that are used to understand how a city is used for a variety of human activities, including agriculture.

The paper examines the variation in land use patterns both in space and time during five different time periods: 1992, 2000, 2008, 2016, and 2024. The aim is to identify the effect on the features of landscapes. The focus on assessing the extent of land use change is an important contribution to the paper. In this environment, indicators such as NDVI, NDWI, and NDBI are used. To demonstrate the change over the eight years, 32 years have been found: 1992, 2000, 2000 2008, 2006, and 2024 were added to highlight the current situation and focus on future prediction.

2. Material and Methods

2.1. Study area

Sargodha City lies in the district of Sargodha in Punjab, Pakistan as shown in Figure 1. It extends between latitudes 31°34' to 32°36' north and longitudes 72°10' to 73°18' east. This is a central district, in the Chaj Doab, the fertile area which separates the Jhelum from the Chenab Rivers (Mobeen et al., 2017). The prevailing land is flat and fertile, making it very conducive for plant growth. The height of these hills ranges between 150 - 200 m (Riaz et al., 2024). A semi-arid climate prevails in the region with hot summer and mild to cool winter. The average summer temperature recorded between 35-42°C, while in winter, it usually remains mild 6-21°C (R. W. Aslam et al., 2024).The population of Sargodha city is 1,872,170 (PBS, 2023).

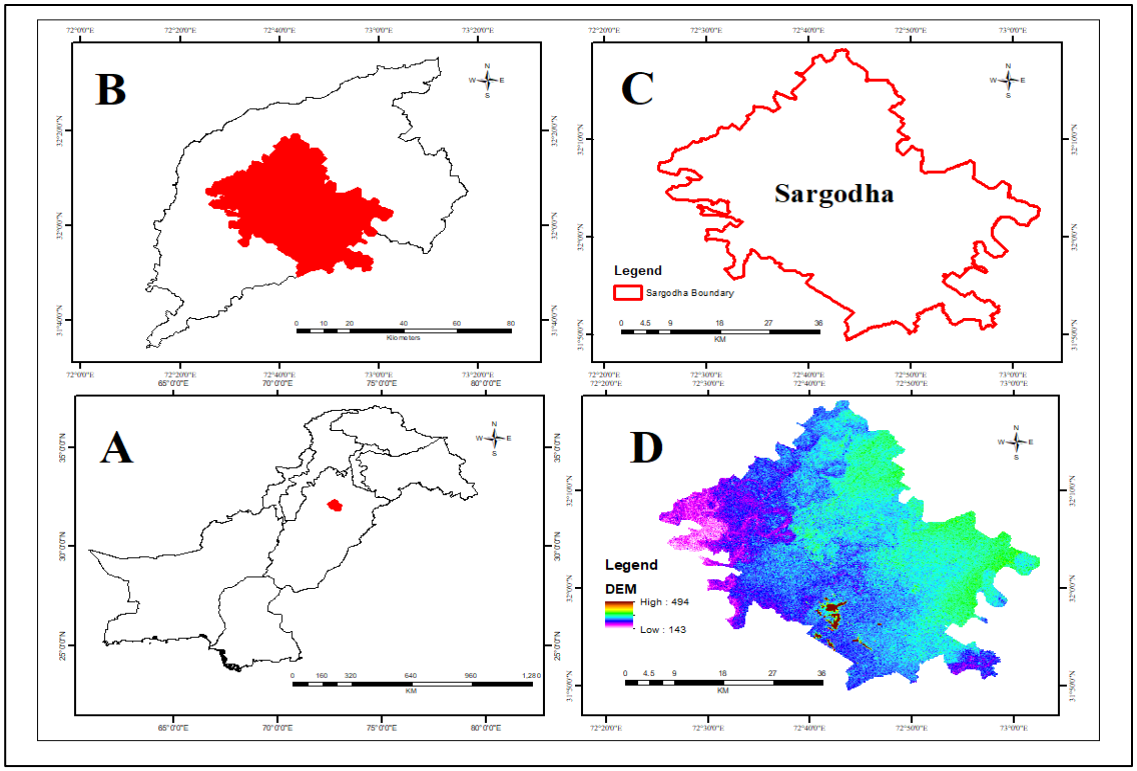


Figure 1. Study Area Map of Sargodha

2.2. Data Acquisition and Land Use Classification

The current study is primarily based on the use of Landsat imagery between 1992 and 2024 as shown in the Figure 2. Appropriate bands were selected to utilize in the generation of the images as shown in Table 1. High-resolution satellite images of Landsat 5 (1992, 2000, 2008), Landsat 8 (2016), and Landsat 9 (2024) were obtained with 30 m resolution. This satellite imagery was used to compute LULC classifications using Random Forest classifier on google earth engine. The land use was categorized in four main classes like urban land which includes predominantly dominated by built-up land, other Land use classes are vegetation, barren land and waterbody. The study also uses various spectral indices to validate the results of land use classification. These spectral indices are normalized difference vegetation index (NDVI), normalized difference built-up index (NDBI) and normalized difference water index (NDWI).

Table 1. Characteristics of Remotely Sensed Data

Sr. #.	Satellite	Sensor	No. of Bands	Year	Radiometric Resolution	Spatial Resolution
1	Landsat 5	TM	7	1992	8 bits	30 m

2	Landsat 5	TM	7	2000	8 bits	30 m
3	Landsat 5	TM	7	2008	8 bits	30 m
4	Landsat 8	OLI/TIRS	11	2016	12 bits	30 m
5	Landsat 9	OLI/TIRS	11	2024	12 bits	30 m

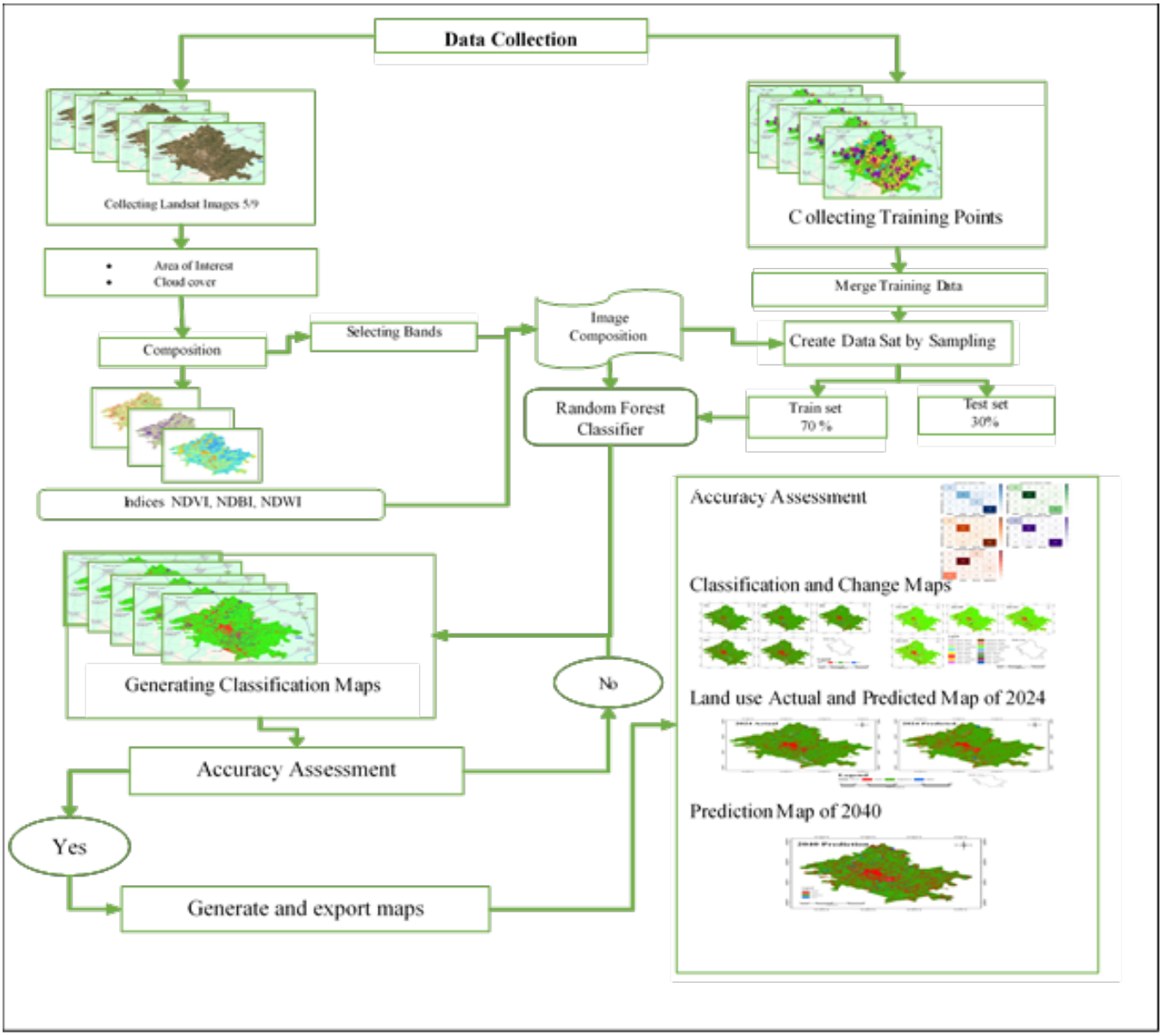


Figure 2. Flow Chart of Methodology

2.3. Accuracy Assessment and Change Detection Analysis

Accuracy assessment is based on the personal knowledge and experience of the observer, ensuring a more reliable output (Pramanik & Punia, 2020). Integrating the random forest (RF) algorithm using Google Earth Engine (GEE) and Landsat data, to achieve 80% accuracy

(Fernando & Senanayake, 2024). The coefficient of the images which are classified by using the google earth engine by applying reference points obtain from the Landsat image with the resolution of 30 m from 1992 to 2024 with gap of 8 years The data was used as a reference for entire research region. About 500 plus points on google earth engine which use randomly by the ratio of 70 to 30 for training and validation points. The kappa coefficient was used to compute accuracy assessment using the following formula.

$$A_p = \frac{p_{ii}}{p+i} \tag{1}$$

$$A_u = \frac{p_{ii}}{p_i} \tag{2}$$

$$A_o = \left(\frac{\sum m_{i-1} p_{ii}}{n}\right) \times 100 \tag{3}$$

$$k = \frac{\sum m_{i=1}\ p_{ii} - \sum c_{i=1}\ p_i + p + \mathrm{i}}{n^2 \sum m_{i=1} p_i + p + i} \tag{4}$$

The above equations are used to measure the accuracy of the classified images. Equation (1) calculates User's Accuracy (A_p), which indicates how well the predicted class on the map matches the ground data. Equation (2) gives Producer's Accuracy (A_u), which is the theme real features are classified to determine how well they classify accurately a feature. The same thing is done by equation (3), which deals with Overall Accuracy (A_o), reflecting the proportion of pixels classified correctly among the total number of classified pixels. Equation (4) is the Kappa Coefficient (κ), which determines the relationship between classified and reference data while correcting random chance. These equations are helpful in validating the classified results' accuracy and reliability. Furthermore, Accuracy, recall, precision, and F1-Score (F1s) were employed to evaluate the end-classified images. These metrics, based on the ratios of True Positive (TP), True Negative (TN), False Positive (FP), and False Negative (FN), provide an informative measure of the classifier's accuracy. As regards accuracy, the ratio of the number of examples correctly classified (TP) to all examples recognized by the algorithm, as provided by Equation 5, is an important parameter for defining the final accuracy evaluation (Soares & Parreiras, 2020).

$$Accuracey = \frac{(true\ positive + true\ negtive\ )}{true\ positive + false\ postive + false\ nagative + true\ nagative} \tag{5}$$

The formula for precision can be written as follows:

$$Precision = \frac{true\ positive}{true\ positive + false\ positive} \quad (6)$$

Recall can be described as the ratio of True Positives to the total number of True Positives and False Negatives (FN). This is illustrated in equation: (Miao & Zhu, 2022).

$$Recall = \frac{true\ positive}{true\ positive + false\ nagative} \quad (7)$$

F1 this measures the model's total performance by combining precision and recall, as seen in equation 8

$$F1 = \frac{(precision \times recall)}{precision + recall} \quad (8)$$

2.4. Land use Change Dynamic and Spectral Indices

An analysis of LULC change was done for 1992–2000, 2000–2008, 2008–2016, and 2016–2024. Cross-tabulation matrices were used in change detection to measure changes in selected land use classes. The standardized method was used to determine the annual rate of change using the equation 9.

$$r = \left[\left(\frac{A2}{A1}\right)^{\frac{1}{t}}\right] - 1 \quad (9)$$

A2 is the area at the end, and A1 is the area at the start, t represents the time between measurements. To further understand the dynamics of land cover shift, each LULC class's net changes, gains, and losses were also calculated (Ullah et al., 2024).

To calculate and validate the variations in LULC changes three different spectral indices like NDVI, NDWI, and NDBI, have been used. These indices were calculated using spectral bands in GEE. The formulas of indices are given below in the Table 2.

Table 2. Derivation of Spectral Indices

NAME	FORMULA	SOURCE
NDVI	$\frac{NIR - R}{NIR + R}$	(Tian et al., 2024)

NDBI	$\frac{MIR_{band-NIR_{band}}}{MIR_{\ band+\ NIR\ band}}$	(Jaswal & Thakur, 2023)
NDWI	$\frac{Green-NIRband}{Green+NIR\ band}$	(Laonamsai et al., 2023)

2.5. Land use change Prediction by Using CA Markov Model

To forecast LULC change dynamics, Markov model and cellular automata, commonly dubbed as the CA–Markov Model was applied. Recent research has been successfully using the model to simulate land use changes since it blends the contiguity of the Markov model with the benefits of cellular automata. This acknowledges the spatial distribution of transitions (Wang et al., 2019). Computing the Markov chain by itself is inadequate for simulating and forecasting landscape dynamics since it does not take into account the spatial distribution of each land category or the spatial direction of development (Ghosh et al., 2017)

$$S_{t,t+1} = P_{(ij)}\, S(t) \tag{10}$$

The CA Markov model transition probability matrix (P) is based on recorded land use changes over a certain time. The matrix is employed in the Markov model to simulate and forecast future landscape patterns; it quantifies the probability of one land cover class changing over time into another (Koko et al., 2020).

$$P_{(ij)} = \begin{bmatrix} P_{11} & P_{12} \ldots\ldots & P_{1n} \\ P_{21} & P_{22} & P_{2n} \\ P_{n1} & P_{n2} & P_{nn} \end{bmatrix} \tag{11}$$

$$0 < P_{(ij)}\, Land \sum_{St+1}{}_{j\,=\,1}^{\,n} P_{(ij)} = 1\ i,j = 1,2 \ldots\ldots n \tag{12}$$

The CA Markov model fundamental elements are grid sizes, cell neighborhoods, cell spaces, time phases, and transition rules. Cells, proximity or close in every dimensional space, may only exist in single state at once, thereby characterizing the properties of the system. Transition rules govern how a cell's state changes with the states of its surroundings.

$$St = \frac{landuse_{(i,t2)} - landuse_{(Ai)}}{landuse_{(i,t1)}} \times \frac{1}{t_2 - t_1} \times 100 \tag{13}$$

Si signifies a change of land use. Land use change during a former time is $landuse_{(Ai)}$ land use change during a subsequent time is $landuse_{(i,t2)}$. $landuse_{(Ai)}$ is the field where, when combined with CA.

3. Results

3.1. LULC Dynamics

The use of accurate and precise classifier is often considered the first step to show how the land use land cover is changing with time. The results show how various types of land use land cover are distributed over space, such as vegetation, urban areas, water bodies, and barren lands, as interpreted from analyzed satellite imagery as shown in the Figure 3. The Classification Maps from 1992-2024 with a Gap of eight years and their statistical explanation are given below.

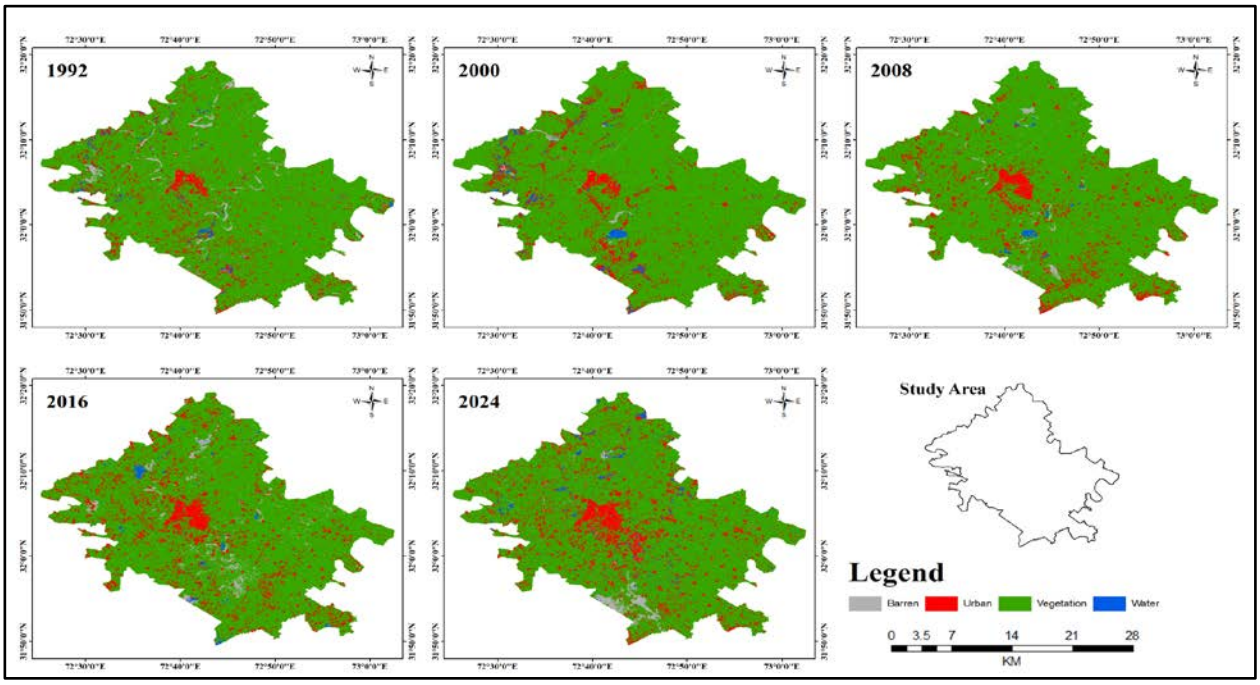


Figure 3. Land Use Land Cover Classification of Sargodha City from 1992-2024

The LULC analysis of Sargodha City (1992-2024) shows remarkable changes in urban extent and vegetation reduction, with slight changes in water and barren land. Urban areas increased from 131 km² (8.5%) in 1992 to 220 km² (14.23%) in 2024, exhibiting fast urbanization. Vegetation cover in Sargodha reduced from 1,356 km² (87.7%) in 1992 to 1,259 km² (81.43%) in 2024, exhibiting a steady but gradual withdrawal. Barren land also receded slightly, from 41

km² (2.6%) in 1992 to 36 km² (2.34%) in 2024, almost unchanged in the long term. Waterbodies in 1992, at 18 km² (1.2%), exhibit a slight increase towards 31 km² (2%) in 2024.

Table 3. Area of Land Use Land Cover from 1992-2024

Years	1992 (km²)	%	2000 (km²)	%	2008 (km²)	%	2016 (km²)	%	2024 (km²)	%
Water	18	1.2	25	1.6	10	0.64	16	1.03	31	2
Urban	131	8.5	144	9.3	159	10.28	201	13	220	14.23
Vegetation	1356	87.7	1369	88.6	1359	87.92	1289	83.4	1259	81.43
Barren	41	2.6	8	0.5	18	1.16	40	2.57	36	2.34
Total	1546	100	1546	100	1546	100	1546	100	1546	100

The land use land cover changes from 1992-2024 in Sargodha City is shown in Table 3. The area under the vegetation has decreased, and the built-up area is almost doubled, indicating a rapid rate of urbanization. In the long term, the condition of the barren land has been mostly stable. The increase in the water bodies is because of the development of fishponds in the region.

3.2. Change detection Analysis based on LULC Maps and Transition Matrix

The change detection analysis is shown in the Figure 4 while the Sankey diagram also helped in to analyze the pattern of land use change from one class to another class as shown in Figure 5. The extent of urban area increased from 131 km² in 1992 to an extent of 220 km² in 2024. However, the most dominant class was vegetation also showed a trend of decline from 1356 km² in 1992 to about 1259 km² in 2024. Waterbody fluctuated from an area of 18 km² to 25 km² from 1992 to 2000, before lessening to about 10 km² in 2008, and recovering again and covering an area of 31 km² by 2024. Barren lands decreased from 41 km² in the year 1992 to about 8 km² in 2000 and increased again to 40 km² by the year 2016, and there has been a slight decrease in barren land to 36 km² by 2024. Between 1992 and 2024, Sargodha City has a substantial land cover changes in as shown in Table 4 by transition matrix values.

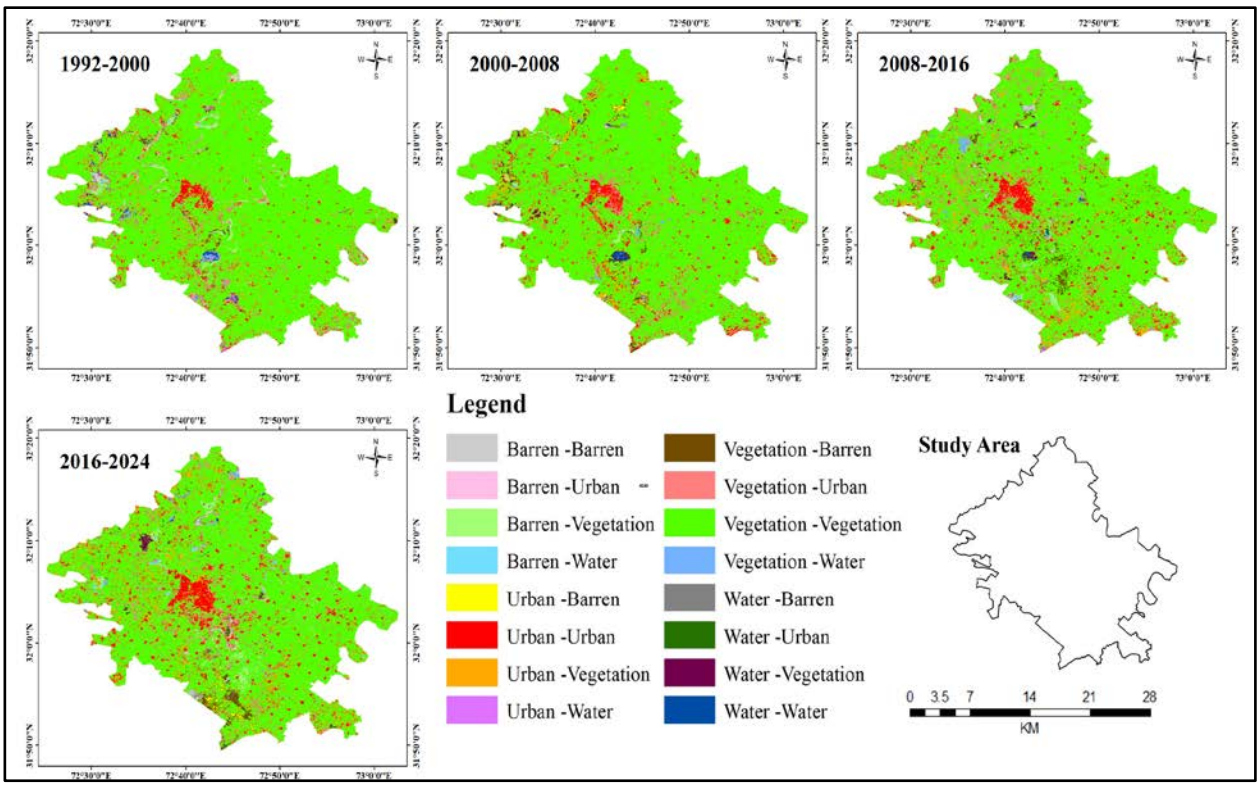


Figure 4. Land Use Change Detection of Classes

Transition Matrix is handy way to analyze the probability of a land use class to transit in other land use class with the passage of time as shown in Table 4. The time period from 1992-2000 is the evident of that vegetal area remained constant while waterbody and barren land experienced the high rate of transition. The 33.3% part of the waterbody and 24.4% of barren land was converted into urban area from 1992-2000. From 2000-2008 the 32% area of the waterbody was converted into the urban area. However, much of the water which was changed to urban land should be considered along with the relatively small size of the water category which is about 18 km^2 in 1992. In this regard, 33.3% of change would account for about 6 km which includes mainly small ponds, seasonal hollows, and wet lands situated on the edge of the urban area. With the development of the urban area, these low lands have been drained, leveled, and used as housing and roads projects which has happened in most rapidly growing cities of Punjab. During this time period vegetation and urban areas were remained stable and showed the less tendency of conversion into other land use classes. From the 2008-2016 vegetation and urban area remained stable while waterbody and barren land were transit into the other land use classes. The dominance of vegetation and barren land is marked with 88.4%

and 44.4% respectively during this time period. From 2016-2024 the stability of urban land use increased from 44.4% to 46%. During the time period waterbody and barren land showed a continuous trend of conversion into vegetation and urban land. About 29.4% of waterbody and 12.9% barren land was converted into urban area from 2016-2024. The most unstable land use classes were waterbody and barren land. Both these classes were significantly converted into other land use classes from 1992 to 2024 while urban area and vegetation remained dominant and stable during this time period.

Table 4. Transition matrix of Sargodha from 1992-2024

1992-2000	**Water**	**Vegetation**	**Barren**	**Urban**	**2000-2008**	**Water**	**Vegetation**	**Barren**	**Urban**
Water	0.389	0.222	0.056	0.333	Water	0.160	0.440	0.080	0.320
Vegetation	0.007	0.928	0.003	0.060	Vegetation	0.002	0.923	0.006	0.069
Barren	0.049	0.659	0.073	0.244	Barren	0.111	0.556	0.222	0.111
Urban	0.046	0.095	0.008	0.351	Urban	0.014	0.056	0.042	0.389
2008-2016	**Water**	**Vegetation**	**Barren**	**Urban**	**2016-2024**	**Water**	**Vegetation**	**Barren**	**Urban**
Water	0.222	0.556	0.111	0.111	Water	0.059	0.471	0.176	0.294
Vegetation	0.005	0.884	0.022	0.089	Vegetation	0.016	0.876	0.017	0.092
Barren	0.105	0.421	0.421	0.053	Barren	0.171	0.634	0.073	0.122
Urban	0.031	0.065	0.019	0.484	Urban	0.015	0.048	0.040	0.460

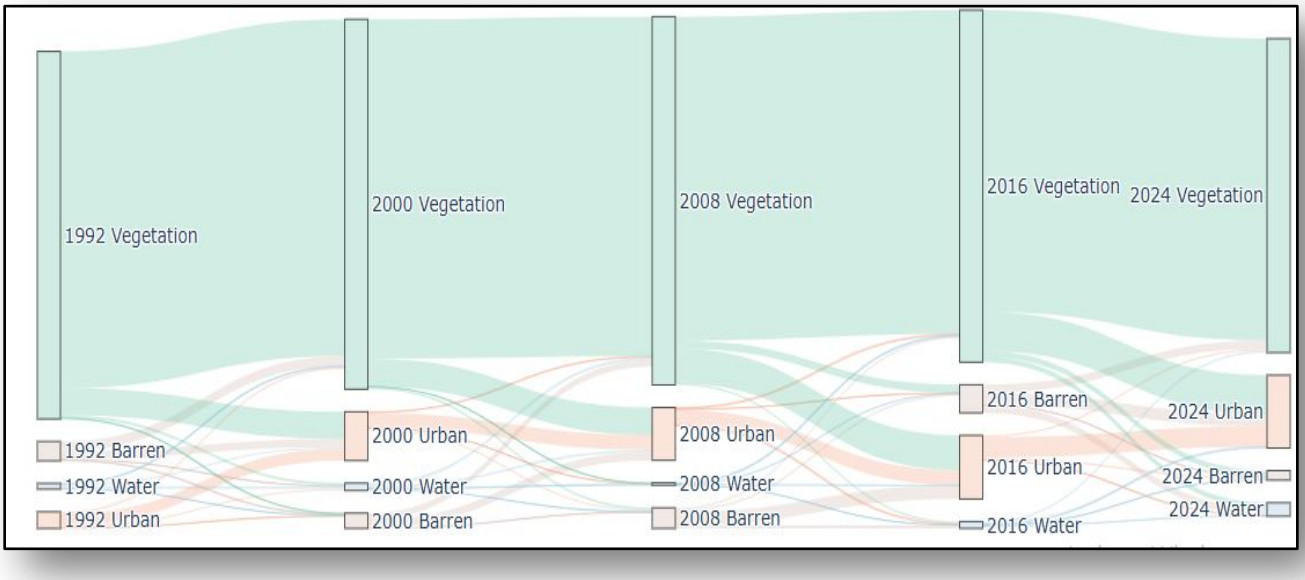


Figure 5. Sankey Diagram of Land Use change 1992 to 2024

3.3. Change Detection Analysis using Spectral Indices

Spectral indices like the Normalized Difference Vegetation Index (NDVI), the Normalized Difference Built-up Index (NDBI), and the Normalized Difference Water Index (NDWI) offer important insights into how landscape changes over time. The current study also utilized the above mentioned spectral indices to strengthen and validate the results of land use land cove classification.

3.4. NDVI (Normalized Vegetation Index)

The NDVI maps for Sargodha City from 1992 to 2024 reveal a noticeable decline in the vegetation cover over time as shown in Figure 6. In 1992 and 2000, the region demonstrated relatively high NDVI values, indicating healthy vegetation, especially in agriculture and forest areas. By 2008, however, the decline in the vegetation cover had become clear, especially in central and southern areas of the city, which is probably due to urban extension and deforestation. The trend continued in 2016, where several fields show lower NDVI values, suggesting ongoing landfall and urbanization. In 2024, a significant reduction in vegetal cover is observed, as several areas of the city are transition from green to purple, which represents increased in built-up land and reduction in vegetal cover vice versa.

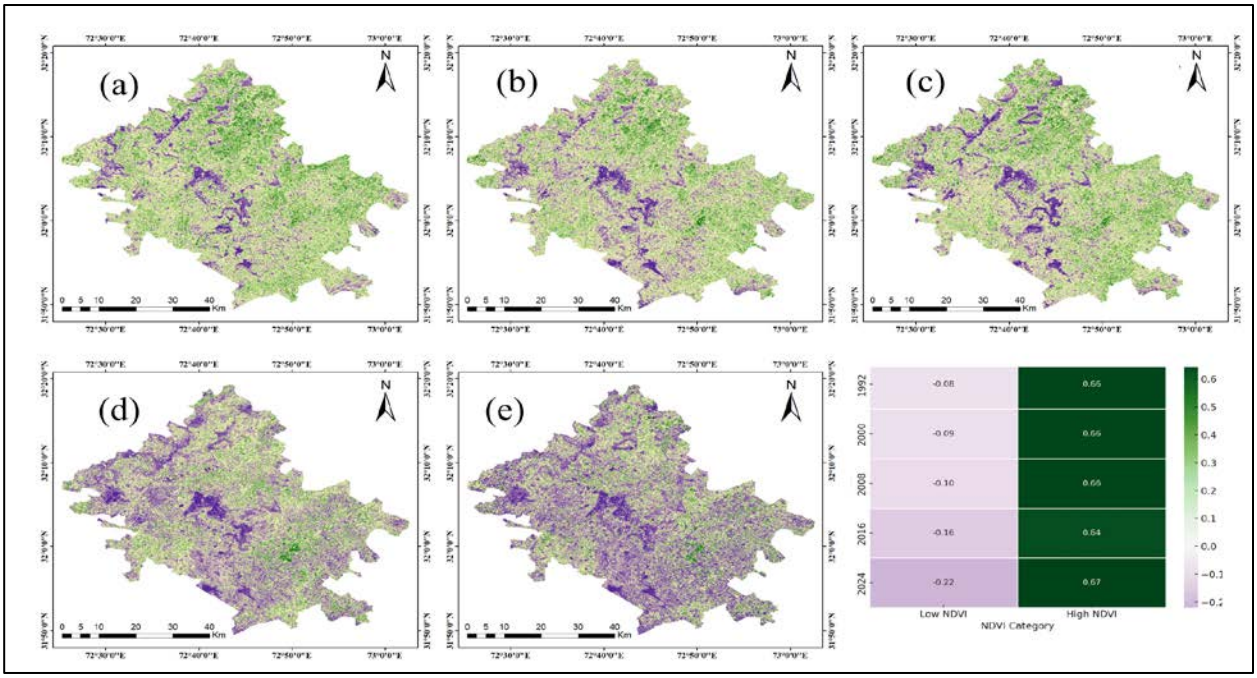


Figure 6. Map of NDVI (Normalized Vegetation Index) from 1992-2024

3.5. NDBI (Normalized Built-up Index)

This set of maps represents generalized differences built-up index for Sargodha City from 1992 to 2024 as shown in Figure 7. NDBI is an important indicator for detecting and analyzing the change in built-up areas, where high value (red) indicates urban expansion, while low value (green) color represents the vegetal areas and water. The Figure 7 represents that in 1992 and 2000, the built-up land was mainly concentrated in small pockets. But after 2008, there has been a noticeable expansion in urban areas, reflecting the ongoing development. In 2016 and 2024, the red regions became wider, indicating the conversion of vegetation or agricultural land by rapid urban growth. The growing trend in NDBI corresponds to the classification of agricultural/land coverage, which confirms expansion of urban areas over the years.

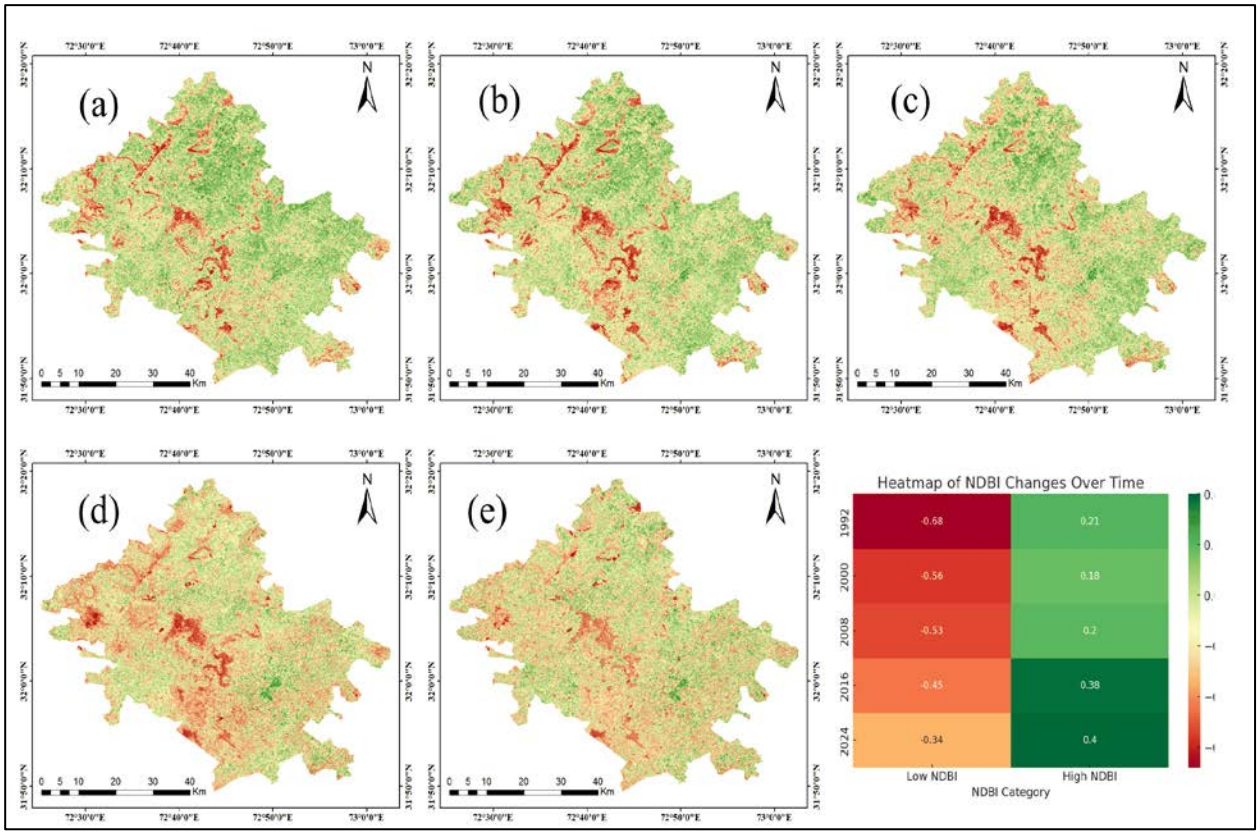


Figure 7. Map of NDBI (Normalized Built-up Index) from 1992-2024

3.6. Accuracy assessment LULC Maps of Sargodha City

Accuracy assessment ensures the credibility of LULC classification by comparing reference data with predicted results. A confusion matrix is employed to compute overall accuracy,

producer's accuracy, user's accuracy, and the kappa coefficient as shown in Figure 8. The Random Forest model was tested with a 70:30 training-to-testing ratios to ensure strong classification. High overall accuracy and kappa values validate the effectiveness of the model in detecting land cover changes. These accuracy metrics improve confidence in the classification outcomes and subsequent LULC predictions. The confusion matrices describe the accuracy of LULC classification from 1992-2024 of selected years. Each matrix compares the classified land category (water, urban, scanty, vegetation) against reference data, which represents properly classified pixels and off-wavic values with diagonal values indicating rescission. The urban class shows a significant increase in properly classified pixels over time, reflecting urban expansion. Vegetation and water categories show rankings in classification accuracy, with remarkable rescission in 2024.

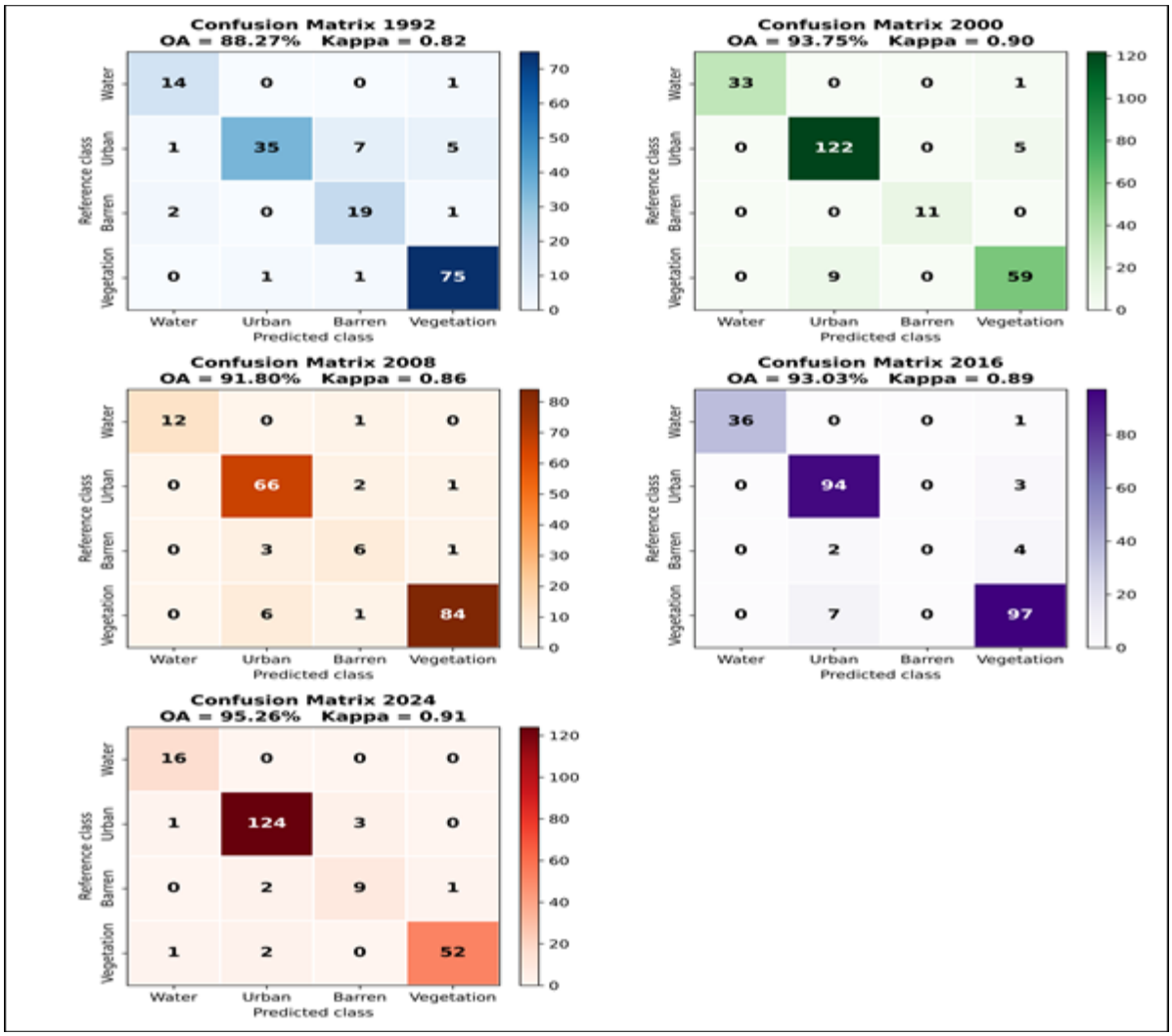


Figure 8. Accuracy assessment of LULC of Sargodha City from 1992-2024

3.7. Land Use Land Cover Modeling of Sargodha City

To ensure its validity and accuracy, it was necessary to check the CA Markov model before forecasting the LULC of 2040 in the Sargodha City. The estimated land cover for model verification 2024 was compared with the actual classified LULC map of 2024. This accuracy assessment consists of overall accuracy calculation, Kappa coefficient computation, and error matrices generation to ensure proper capture of previous land-use changes and classification accuracy by the model. The CA Markov model was applied to 2040, when once successful verification was obtained to analyze the use of land and land cover changes (LULC), so indicates future urban expansion, vegetation changes and environmental effects in Sargodha City.

3.8. CA-Markov Method Validation

The difference in the actual and forecasted LULC maps for 2024 shows that CA/Markov model can accurately reproduce the usual land cover patterns, and can predict more accurately the spatial distributions as shown in Figure 9. More than 97% accuracy of the CA/Markov model has proven its reliability in forecasting LULC changes, so it is a useful tool in environmental management and urban planning.

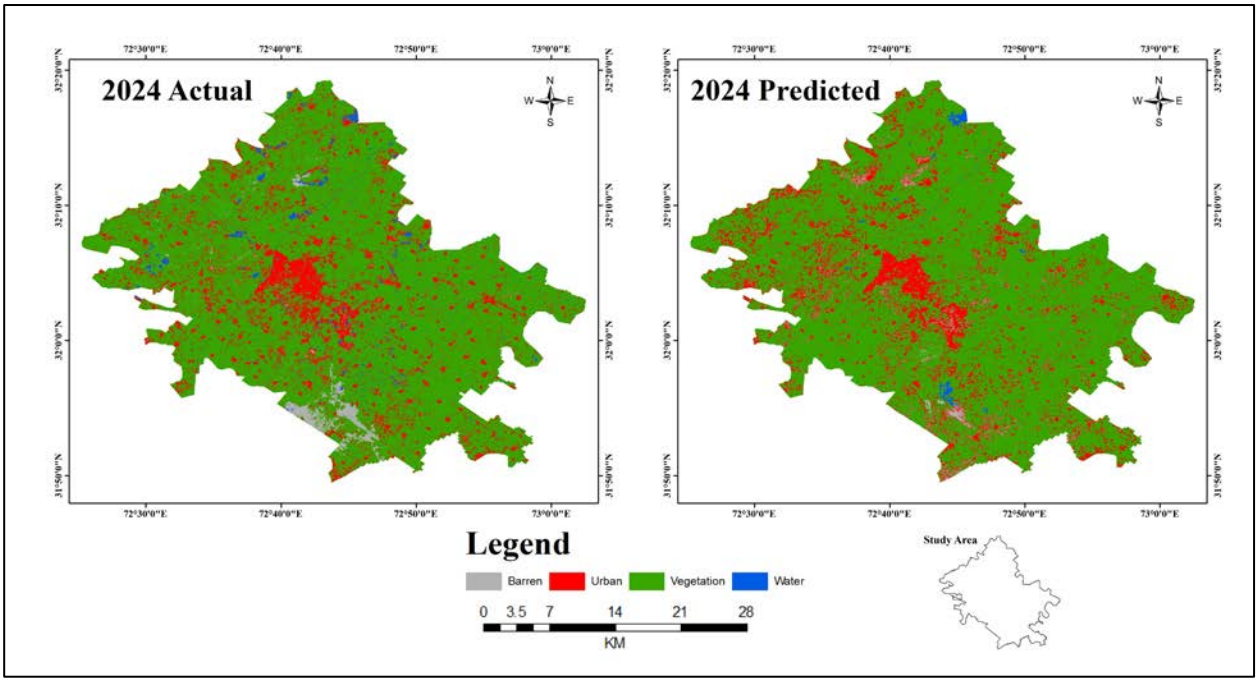


Figure 9. Comparison of Actual and Predicted Map of Sargodha City of 2024

By comparing the actual LULC of 2024 with a forecasted LULC of 2024 it was observed that the CA Markov model precisely and accurately forecast the changes in land use/land cover (LULC) of Sargodha City in 2024 as shown in Table 5. The data shows that the vegetation is remained constant covering an area of 1259 km² (81.43%), hence the model is accurate in forecasting this category. The addition of urban areas is responsible for the expected increase to 240 km² (15.53%) from the present 220 km² (14.23%). Waterbody has shown an obvious change when the model predicts this land use class in 2024 while barren land remains more or less constant with just an increase of 37 km² (2.39%) to 40 km² (2.59%) in 2024 predicted map of LULC as compared to the actual classified map of the study area.

Table 5. Output Actual and Predicted Map of LULC (2024)

Class Type	LULC Actual	(%)	LULC Predicted	(%)
Vegetation	1259	81.43	1259	81.43
Urban	220	14.23	240	15.53
Water	31	1.96	7	0.45
Barren	37	2.39	40	2.59

3.9. Modeling of Land Use Land Cover Change (2040)

The Markov model forecasts incoming changes on the basis of past land use/land cover (LULC) patterns. This models were used to develop the map for 2040 as shown in the Figure 10. This model assesses the probable transitions between land cover classes, estimates spatial changes over time. The results indicate massive urban increase, loss of vegetation cover, and minor changes to water bodies.

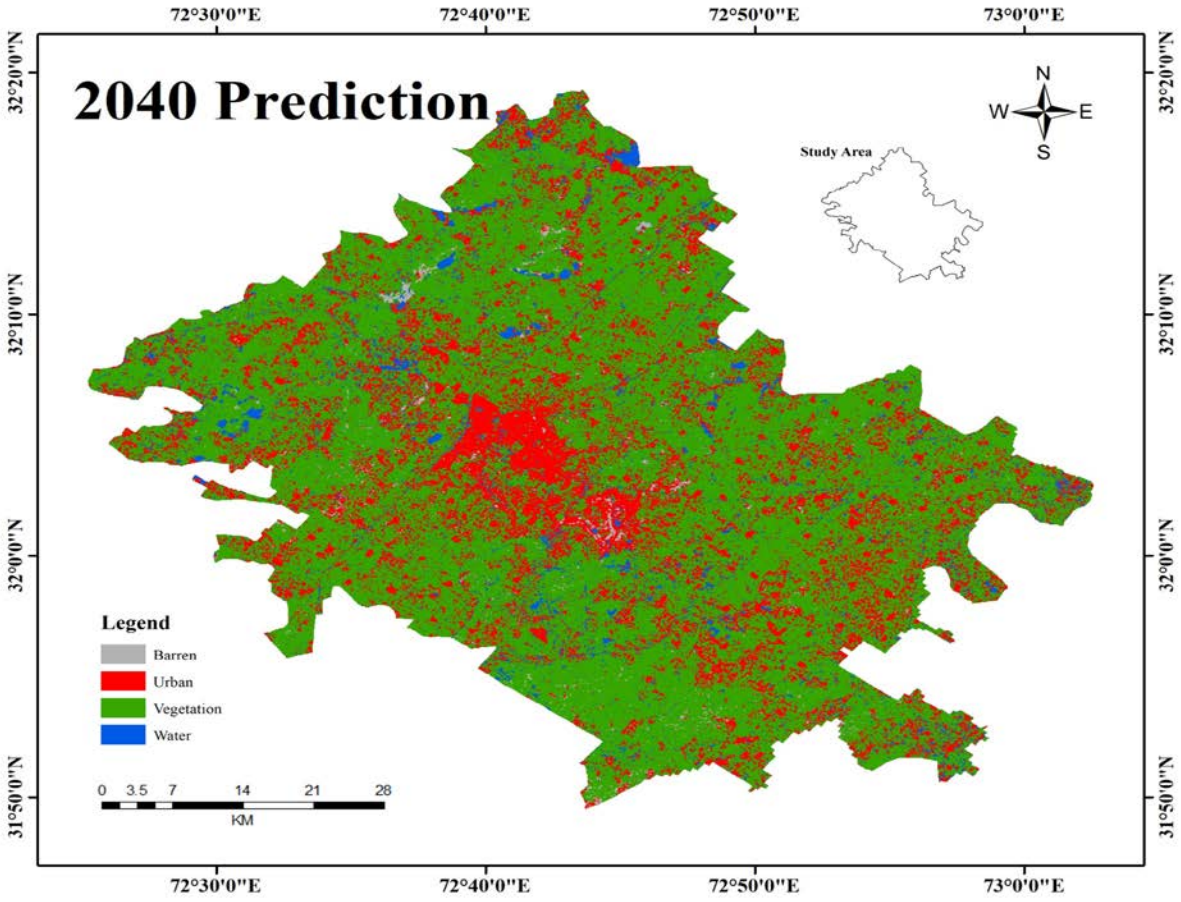


Figure 10. Predicted Map of 2040

3.10. Change Detection in LULC from 2024-2040

The transition matrices for LULC changes between 2024 and 2040 give the probabilities of land classes transitioning into other classes over time as shown in Table 6. Water has a 45.1% probability to remain as water, a 35.4% chance to be converted to vegetation, a 3.2% chance to become barren land, and a 16% chance of urban land use. Vegetation is presumed to survive at a probability of 75.7%, while 5.4% of the vegetation cover may convert into a water body, 0.7% into barren, and 18.1% into urban area. On the other hand, bare land has an era of great functional transitions: 70.3% goes to vegetation, 5.4% to water, 8.1% stays barren, and 16.2% becomes urban area in 2040. An urban environment is the most stable, with 50.9% of its remaining in an urban environment; 4% could become water, 1.3% vegetation, and 3.6% barren. This table represents an increase in the area of man-made land while there is a decrease in the area of bare land.

Table 6. Transition Matrix of Land Use Land Cover from 2024-2040

2024-2040	Water	Vegetation	Barren	Urban
Water	0.451	0.354	0.032	0.16
Vegetation	0.054	0.75695	0.007	0.181
Barren	0.054	0.702703	0.081	0.162
Urban	0.040	0.013	0.036	0.509

The Sankey diagram shows how land use and land cover (LULC) will change from 2024 to 2040 as shown in Figure 11. The figure below represents that vegetal cover will be converted into the urban area by the end of 2040 in Sargodha City.

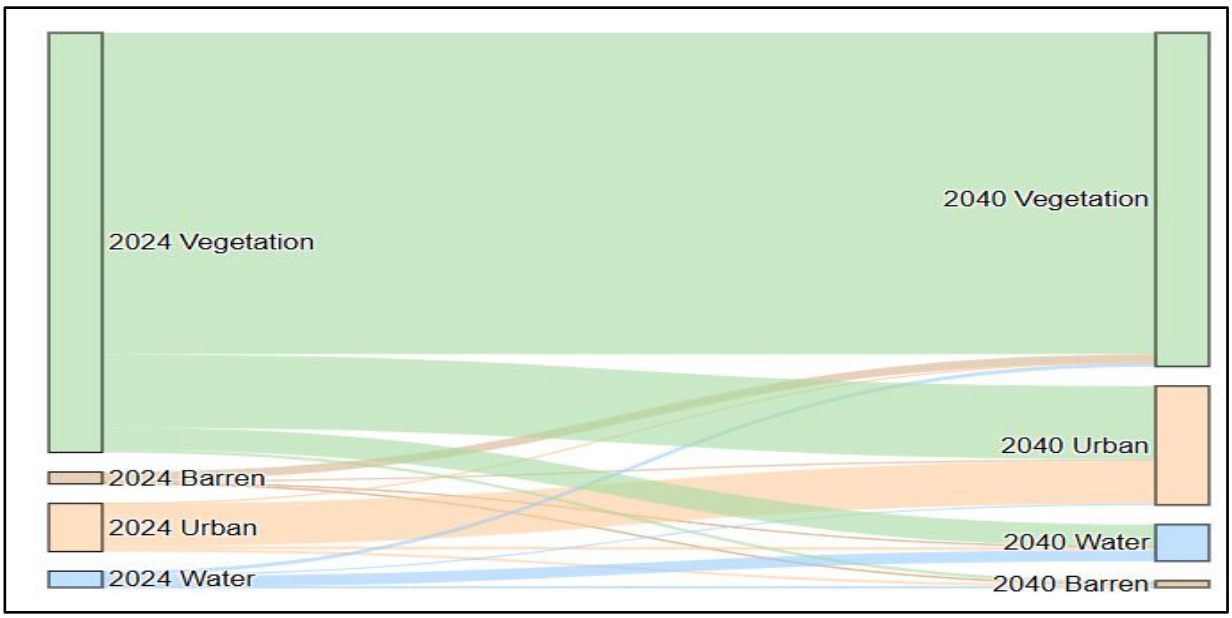


Figure 11. Sankey diagram of Land Use and Land Cover Change from 2024 to 2040

The land use and land cover (LULC) shift from 2024 to 2040 shows a significant change in the growth of city at the expense of reduction in green spaces as show in Table 7. The output of CA-Markov Model suggest that the built-up area of Sargodha City will be 351 km² (22.69%) in 2040 pointing out the rapid urban development. Green areas shrink from 1259 km² (81.43%) to 1080 km² (69.85%), as people turn this land into cities or use it for other things. Water bodies grow from 31 km² (2%) to 94 km² (6.09%) due to natural changes or tries to reclaim land. Empty land drops from 36 km² (2.34%) to 21 km² (1.37%) showing efforts to make use of this land. These shifts show how land cover keeps changing highlighting the need for smart planning to make sure city growth doesn't harm nature.

Table 7. Area under each land use in 2024 and 2040

Years	**2024 (**km²)	%	**2040 (**km²)	%
Water	31	2	94	6.09
Urban	220	14.23	351	22.69
Vegetation	1259	81.43	1080	69.85
Barren	36	2.34	21	1.37
Total	1546	100	1546	100

4. Discussion and Conclusions

The expansion of the urbanized area in Sargodha city reached 67.9%, from 131 km² in 1992 to 220 km² in 2024, while there was an almost 97 km² loss of vegetation area in the same period. Such expansion is consistent with the 41.9% rise in the population density of the district and supports the previous research on urban sprawl in Sargodha. Similarly, in terms of conversion of cropland to urban area, losses of similar magnitude were noticed in Okara. Multan and Lahore. Water and barren land are the least stable classes in the study. Inland water bodies were filled up with construction activities, whereas increase in water class post-2008 was due to fish pond constructions. Decline in NDVI with an increase in NDBI in peri-urban regions provided supporting evidence of this finding. The classification resulted in overall accuracy between 88.27% and 95.26% and Kappa index between 0.82 and 0.91. These numbers can be compared with the results obtained from other studies based on random forest classification together with CA–Markov modeling. There are two limitations worth mentioning here. The first one is related to the variation in image quality from historical Landsat images that may impact the classification of smaller classes. The second limitation lies in the CA–Markov projections that always assume future continuation of trends observed in the past.

This research used Google Earth Engine, random forest classifier, spectral indices, and the CA-Markov model to examine land-use/land-cover changes in Sargodha City between 1992 and 2024 and predict the same up to 2040. The following were some of the main conclusions drawn from this study:

1. There has been a significant increase in the built-up area from 131 km² (8.5%) in 1992 to 220 km² (14.23%) in 2024. There has been a corresponding decrease in vegetation area from 1356 km² (87.7%) to 1259 km² (81.43%).
2. Water and barren land were identified as the two most dynamic classes being converted to either urban or agricultural use.
3. According to the trend witnessed, the built-up land would grow to 351 km² (22.69%) in 2040 while vegetation area would decline to 1080 km² (69.85%).

The above conclusions present a number of implications regarding land-use planning in Sargodha as follows:

There should be an urban growth boundary established as part of the city master plan for preventing the conversion of productive agricultural land at the fringes of the city. Private housing schemes should be more closely controlled and monitored as they are the major cause

of fringe expansion. Encourage infill development and vertical expansion rather than sprawling. Wetlands, ponds, and other low-lying drainage areas should be protected against filling activities. Create greenbelts and urban green spaces.

References

Ashraf, H., Mobeen, M., Miandad, M., Khan, M. A., Rahman, G., & Munawar, S. (2022). Assessment of urban sprawl in sargodha city using remotely sense data. Ecological Questions, 33(4), 131-140.

Ashraf, H., Rahman, G., Khan, M. A., Ul Moazzam, M. F., & Miandad, M. (2023). Spatio-temporal urban sprawl of sargodha city, Punjab, Pakistan, [in:] Urban Environment and Smart Cities in Asian Countries: Insights for Social, Ecological, and Technological Sustainability, pp. 543-560, Springer.

Aslam, A. (2024). Impacts of Urbanization on Agricultural Land in Multan District: Past and Future Trend Analysis Using Remote Sensing Approach. Institute of Geographical Information Systems (IGIS), Pakistan.

Aslam, R. W., Shu, H., Tariq, A., Naz, I., Ahmad, M. N., Quddoos, A., . . . Aeman, H. (2024). Monitoring landuse change in Uchhali and Khabeki wetland lakes, Pakistan using remote sensing data. Gondwana Research, 129, 252-267.

Aylett, A., Joeman, B. D., Lefevre, B., Luque-Ayala, A., Rahman, A., Roberts, D., . . . Watkins, M. (2015). Climate change mitigation in rapidly developing cities, [in:] The Routledge Handbook of Urbanization and Global Environmental Change, pp. 549-560, Routledge.

Butt, A., Shabbir, R., Ahmad, S. S., & Aziz, N. (2015). Land use change mapping and analysis using Remote Sensing and GIS: A case study of Simly watershed, Islamabad, Pakistan. The Egyptian journal of remote sensing and space science, 18(2), 251-259.

Cao, Q., Liu, Y., Georgescu, M., & Wu, J. (2020). Impacts of landscape changes on local and regional climate: A systematic review. Landscape Ecology, 35, 1269-1290.

Chen, Q., Chen, H., Zhang, J., Hou, Y., Shen, M., Chen, J., & Xu, C. (2020). Impacts of climate change and LULC change on runoff in the Jinsha River Basin. Journal of Geographical Sciences, 30, 85-102.

Farhan, M., Wu, T., Amin, M., Tariq, A., Guluzade, R., & Alzahrani, H. (2024). Monitoring and prediction of the LULC change dynamics using time series remote sensing data with Google Earth Engine. Physics and Chemistry of the Earth, Parts a/b/c, 136, 103689.

Farooq, M. U., Riaz, O., Khalid, M., & Qazi, B. D. M. N. (2024). Relationship between Population Attributes and Built-up Area Expansion in Sargodha District, Pakistan. OEconomia.

Fernando, W. A. M., & Senanayake, I. (2024). Developing a two-decadal time-record of rice field maps using Landsat-derived multi-index image collections with a random forest classifier: A Google Earth Engine based approach. Information Processing in Agriculture, 11(2), 260-275.

Fu, F., Deng, S., Wu, D., Liu, W., & Bai, Z. (2022). Research on the spatiotemporal evolution of land use landscape pattern in a county area based on CA-Markov model. Sustainable Cities and Society, 80, 103760.

Gao, Y., Li, M., & Jiang, P. (2020). Land-type mapping and its application to land-use zoning: A case study of Jiangsu province, eastern China. Journal of Maps, 16(2), 847-854.

Ghosh, P., Mukhopadhyay, A., Chanda, A., Mondal, P., Akhand, A., Mukherjee, S., . . . Ghosh, T. (2017). Application of Cellular automata and Markov-chain model in geospatial environmental modeling-A review. Remote Sensing Applications: Society and Environment, 5, 64-77.

Gu, D., Andreev, K., & Dupre, M. E. (2021). Major trends in population growth around the world. China CDC weekly, 3(28), 604.

Guha, S., Govil, H., Gill, N., & Dey, A. (2020). Analytical study on the relationship between land surface temperature and land use/land cover indices. Annals of GIS, 26(2), 201-216.

Hailu, A., Mammo, S., & Kidane, M. (2020). Dynamics of land use, land cover change trend and its drivers in Jimma Geneti District, Western Ethiopia. Land use policy, 99, 105011.

Hashim, M., Atta-ur-Rahman, M. Q., Farooq, M. U., Nadeem, B., & Muneer, S. (2023). Determination Of Demographic Change And Urban Settlement Pattern In Multan City, Pakistan. Journal of Positive School Psychology, 7(6), 1243-1253.

Hossain, M. I., & Rahman, M. M. (2024). Assessing the Rapid Urbanization in Tertiary City of Bangladesh by Land Use and Land Cover Change Detection from 2000 to 2024 through NDVI Based Classification and future forecasting for 2032 by Cellular Automata (CA) model in Meherpur District.

Huang, S., Tang, L., Hupy, J. P., Wang, Y., & Shao, G. (2021). A commentary review on the use of normalized difference vegetation index (NDVI) in the era of popular remote sensing. Journal of Forestry Research, 32(1), 1-6.

Hussain, S., Mubeen, M., & Karuppannan, S. (2022). Land use and land cover (LULC) change analysis using TM, ETM+ and OLI Landsat images in district of Okara, Punjab, Pakistan. Physics and Chemistry of the Earth, Parts a/b/c, 126, 103117.

Jaber, S. M. (2021). On the relationship between normalized difference vegetation index and land surface temperature: MODIS-based analysis in a semi-arid to arid environment. Geocarto International, 36(10), 1117-1135.

Jamei, Y., Seyedmahmoudian, M., Jamei, E., Horan, B., Mekhilef, S., & Stojcevski, A. (2022). Investigating the relationship between land use/land cover change and land surface temperature using Google Earth engine; case study: Melbourne, Australia. Sustainability, 14(22), 14868.

Jaswal, S., & Thakur, P. (2023). Correlation between LST, NDVI and NDBI with reference to Urban Sprawling–A Case Study of Shimla city. Int. J. Multidiscip Res, 5, 1-14.

Jatoi, F. Z. (2021). Agriculture in Pakistan and its impact on Economic growth. Available at SSRN.

Jothimani, M., Gunalan, J., Duraisamy, R., & Abebe, A. (2021). Study the Relationship Between LULC, LST, NDVI, NDWI and NDBI in Greater Arba Minch Area, Rift Valley, Ethiopia. Paper presented at the 3rd International Conference on Integrated Intelligent Computing Communication & Security (ICIIC 2021).

Kabisch, N., Selsam, P., Kirsten, T., Lausch, A., & Bumberger, J. (2019). A multi-sensor and multi-temporal remote sensing approach to detect land cover change dynamics in heterogeneous urban landscapes. Ecological Indicators, 99, 273-282.

Khanal, S., Kc, K., Fulton, J. P., Shearer, S., & Ozkan, E. (2020). Remote sensing in agriculture—accomplishments, limitations, and opportunities. Remote sensing, 12(22), 3783.

Khine, M. M., Maw, Y. Y., & Win, K. M. M. (2018). Change analysis of indices (NDWI, NDVI, NDBI) for Mawlamyine City area using google earth engine. J. Myanmar Acad. Arts Sci, 16(5).

Koko, A. F., Han, Z., Wu, Y., Abubakar, G. A., & Bello, M. (2022). Spatiotemporal land use/land cover mapping and prediction based on hybrid modeling approach: a case study of Kano Metropolis, Nigeria (2020–2050). Remote sensing, 14(23), 6083.

Koko, A. F., Yue, W., Abubakar, G. A., Hamed, R., & Alabsi, A. A. N. (2020). Monitoring and predicting spatio-temporal land use/land cover changes in Zaria City, Nigeria, through an integrated cellular automata and markov chain model (CA-Markov). Sustainability, 12(24), 10452.

Laonamsai, J., Julphunthong, P., Saprathet, T., Kimmany, B., Ganchanasuragit, T., Chomcheawchan, P., & Tomun, N. (2023). Utilizing NDWI, MNDWI, SAVI, WRI, and AWEI for estimating erosion and deposition in Ping River in Thailand. Hydrology, 10(3), 70.

Manna, H., Sarkar, S., Hossain, M., & Dolui, M. (2024). Modeling and predicting spatio-temporal land use land cover changes and urban sprawling in Kalaburagi City Corporation, Karnataka, India: a geospatial analysis. Modeling Earth Systems and Environment, 10(1), 809-832.

Mansour, S., Al-Belushi, M., & Al-Awadhi, T. (2020). Monitoring land use and land cover changes in the mountainous cities of Oman using GIS and CA-Markov modelling techniques. Land use policy, 91, 104414.

Miao, J., & Zhu, W. (2022). Precision–recall curve (PRC) classification trees. Evolutionary intelligence, 15(3), 1545-1569.

Mobeen, M., Ahmed, H., Ullah, F., Riaz, M. O., Mustafa, I., Khan, M. R., & Hanif, M. U. (2017). Impact of climate change on the precipitation pattern of district Sargodha, Pakistan. International Journal of Climate Change Strategies and Management, 9(1), 21-35.

Naikoo, M. W., Rihan, M., & Ishtiaque, M. (2020). Analyses of land use land cover (LULC) change and built-up expansion in the suburb of a metropolitan city: Spatio-temporal analysis of Delhi NCR using landsat datasets. Journal of Urban Management, 9(3), 347-359.

Nuissl, H., & Siedentop, S. (2021). Urbanisation and land use change. Sustainable land management in a European context: a co-design approach, 75-99.

PBS. (2023). Pakistan Bureau of Statistics 2023 census data of Pakistan. https://www.pbs.gov.pk

Peng, X., Zegen, W., Zhuo, H., Zhiwei, Y., Rui, L., & Yang, Z. (2023). A land degradation assessment based on the combination of quantitative and qualitative change of land cover: a case study in Pakistan. Environmental Earth Sciences, 82(1), 43.

Pramanik, S., & Punia, M. (2020). Land use/land cover change and surface urban heat island intensity: source–sink landscape-based study in Delhi, India. Environment, Development and Sustainability, 22, 7331-7356.

Riaz, M. O., Younis, U., Khalid, M., Umar, M., & Hashim, M. (2024). A Spatio Temporal Comparative Analysis of Land Use Land Cover Change (LULC) between Sargodha District and Kaghan Valley, Pakistan. OEconomia.

Roy, K. C., Soren, D. D. L., & Biswas, B. (2024). Land-use/cover change and future prediction by integrating the ML techniques of random forest and CA-Markov chain model of the Ganges alluvial tract of Eastern India. Environment, Development and Sustainability, 1-28.

Sameer, M., Malik, K., & Gulzar, R. (2025). Spatial and temporal analysis of land use land cover changes in Sargodha district Punjab. ASSAJ, 3(01), 194-204.

Sampath, V. K., & Radhakrishnan, N. (2024). Prediction of soil erosion and sediment yield in an ungauged basin based on land use land cover changes. Environmental Monitoring and Assessment, 196(1), 56.

Soares, M. A. C., & Parreiras, F. S. (2020). A literature review on question answering techniques, paradigms and systems. Journal of King Saud University-Computer and Information Sciences, 32(6), 635-646.

Tassi, A., & Vizzari, M. (2020). Object-oriented lulc classification in google earth engine combining snic, glcm, and machine learning algorithms. Remote sensing, 12(22), 3776.

Tian, J., Tian, Y., Wan, W., Yuan, C., Liu, K., & Wang, Y. (2024). Research on the Temporal and Spatial Changes and Driving Forces of Rice Fields Based on the NDVI Difference Method. Agriculture, 14(7), 1165.

Tichý, L., Hennekens, S. M., Novák, P., Rodwell, J. S., Schaminée, J. H., & Chytrý, M. (2020). Optimal transformation of species cover for vegetation classification. Applied Vegetation Science, 23(4), 710-717.

Ullah, S., Abbas, M., & Qiao, X. (2024). Impact assessment of land-use alteration on land surface temperature in Kabul using machine learning algorithm. Journal of Spatial Science, 1-23.

United Nations, D. f. E. a. S. A. (2019). World population prospects 2019: Highlights (ST/ESA/SER.A/423). Retrieved from New York, NY.

Verma, P., Raghubanshi, A., Srivastava, P. K., & Raghubanshi, A. (2020). Appraisal of kappa-based metrics and disagreement indices of accuracy assessment for parametric and nonparametric techniques used in LULC classification and change detection. Modeling Earth Systems and Environment, 6, 1045-1059.

Wang, M., Cai, L., Xu, H., & Zhao, S. (2019). Predicting land use changes in northern China using logistic regression, cellular automata, and a Markov model. Arabian Journal of Geosciences, 12(24), 790.

Winkler, K., Fuchs, R., Rounsevell, M., & Herold, M. (2021). Global land use changes are four times greater than previously estimated. Nature communications, 12(1), 2501.

Xiang, M., Yang, J., Li, W., Song, Y., Wang, C., Liu, Y., . . . Tan, Y. (2022). Spatiotemporal evolution and simulation prediction of ecosystem service function in the western Sichuan plateau based on land use changes. Frontiers in Environmental Science, 10, 890580.

Yaghoobi, M., Vafaeenejad, A., Moradi, H., & Hashemi, H. (2022). Analysis of landscape composition and configuration based on LULC change modeling. Sustainability, 14(20), 13070.

Yar, P., & Huafu, J. (2019). Horizontal development of built-up area and its impacts on the agricultural land of Peshawar city district (1991–2014). Journal of the Indian Society of Remote Sensing, 47, 1537-1545.

Zhao, Q., Yu, L., Li, X., Peng, D., Zhang, Y., & Gong, P. (2021). Progress and trends in the application of Google Earth and Google Earth Engine. Remote sensing, 13(18), 3778.

Zhou, L., Dang, X., Sun, Q., & Wang, S. (2020). Multi-scenario simulation of urban land change in Shanghai by random forest and CA-Markov model. Sustainable Cities and Society, 55, 102045.